A volcanotectonic cascade: Activation of range front faulting and eruptions by dike intrusion, Mono Basin-Long Valley Caldera, California

M. Bursik,[1] C. Renshaw,[2] J. McCalpin,[3] and M. Berry[4]

Received 17 June 2002; revised 10 February 2003; accepted 25 March 2003; published 23 August 2003.

[1] Stratigraphic data suggest that during the North Mono-Inyo eruption sequence of ~1350 A.D. a series of strong earthquakes occurred near the end of the North Mono explosive phases and the beginning of the Inyo explosive phases. The temporal proximity of these events suggests the possibility of a causal relationship. Geological and geomorphic features of the Hartley Springs Fault are consistent with rupture of the fault during the eruption sequence. These features include steep central slope segments on several fault scarps and a fault scarp and stratigraphic offset since the deposition of ~1200-year-old tephra. We hypothesize that the Inyo Dike, found by drilling underneath the main Inyo vents, neared the Hartley Springs Fault as it propagated southward from the Mono Basin circa 1350 A.D. We demonstrate that once the lateral distance between dike and fault was sufficiently small, the mechanical interaction between them could have triggered the slip observed on the fault. The slip, in turn, could have reduced the horizontal confining pressure in a region near the southern tip of the fault. The presence of the main Inyo vents in this region suggests that the reduction in confining stress was sufficient to allow magma to propagate to the surface. The results suggest that a volcanotectonic "cascade" of eruptions and earthquakes is a possible mechanism by which a large section of a range front or rift system can be activated because of the positive feedback provided by each element to continued activity. *INDEX TERMS:* 7221 Seismology: Paleoseismology; 8109 Tectonophysics: Continental tectonics—extensional (0905); 8145 Tectonophysics: Physics of magma and magma bodies; 8434 Volcanology: Magma migration; 8414 Volcanology: Eruption mechanisms; *KEYWORDS:* Long Valley caldera, Mono Craters, Inyo Domes, dikes, volcano-tectonic structure, volcanic earthquakes

Citation: Bursik, M., C. Renshaw, J. McCalpin, and M. Berry, A volcanotectonic cascade: Activation of range front faulting and eruptions by dike intrusion, Mono Basin-Long Valley Caldera, California, *J. Geophys. Res.*, *108*(B8), 2393, doi:10.1029/2002JB002032, 2003.

1. Introduction

[2] In May 1980, four *M* 6 earthquakes shook Long Valley Caldera, California. Continued earthquake swarms and other symptoms of volcanic unrest have made it important to maintain a substantial monitoring effort at Long Valley [*Rundle and Hill*, 1988]. This effort has resulted in the observation of myriad tectonic earthquakes in association with indicators of magmatic movement. Several workers have articulated models linking the tectonic and magmatic systems. *Hill* [1977] and *Vetter* [1984] hypothesized that small tectonic earthquakes within a complex network of faults and fissures serve to pump magma into the fissures due to the pressure changes induced by fault movement. *Savage and Clark* [1982] hypothesized that the 1980 earthquakes themselves resulted directly from magmatic resurgence in the Long Valley chamber. *Bursik and Sieh* [1989] hypothesized that both rupture along normal faults and the intrusion of dikes are responses to the regional stretching of the crust in this portion of the western Basin Ranges. Where magma is available, crustal stretching is preferentially accommodated by dike intrusion.

[3] Pyroclastic fall, flow and surge beds, as well as viscous high-silica rhyolite domes, erupted from a dike during the North Mono eruption sequence [*Sieh and Bursik*, 1986]. The pyroclastic phases of this eruption most likely occurred during the interval 1325 to 1368 A.D. The Inyo vents, 15 km to the south of the North Mono vents, became active with eruption of the South Deadman tephra sometime before 1369 A.D. (Figure 1) [*Miller*, 1985]. For simplicity, these eruptions will be referred to together as the 1350 A.D.

[1]Department of Geology, State University of New York at Buffalo, Buffalo, New York, USA.
[2]Department of Earth Sciences, Dartmouth College, Hanover, New Hampshire, USA.
[3]GEO-HAZ Consulting, Inc., Crestone, Colorado, USA.
[4]Evergreen, Colorado, USA.

0148-0227/03/2002JB002032$09.00

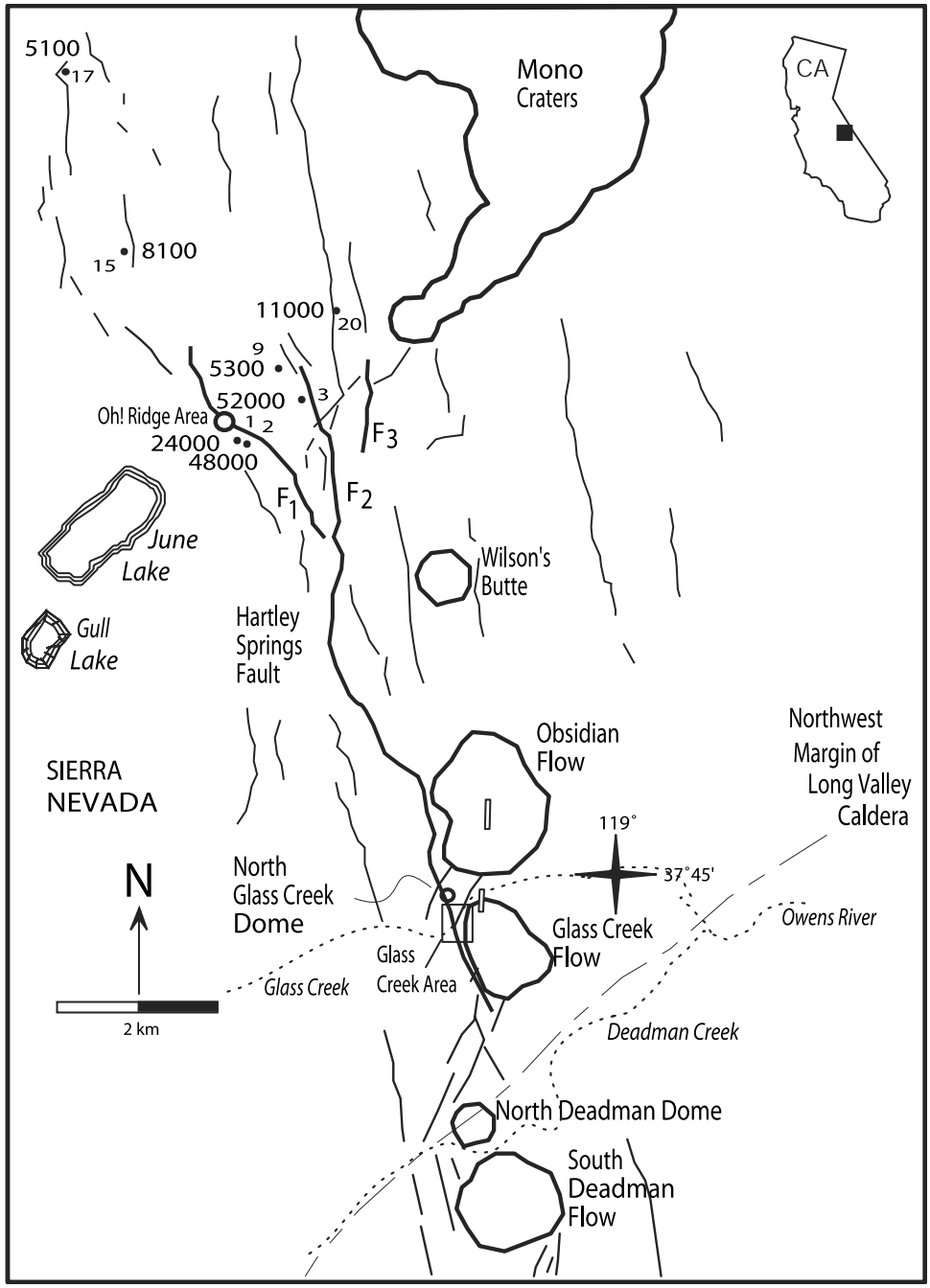

Figure 1. Location map of the Hartley Springs Fault-southern Mono Craters-Inyo Domes area. The location of trench sites at Oh! Ridge are indicated with a circle and labeled "Oh! Ridge area." The location of the 200 × 400 m study area at Glass Creek is indicated with a box labeled "Glass Creek area." Prominent fault scarps and fissures are mapped as lines [from *Fink*, 1985; *Bursik and Sieh*, 1989], with the strands of the Hartley Springs Fault in bold. Domes of the Mono-Inyo chain are outlined and labeled; open rectangles in Obsidian and Glass Creek flows show approximate orientation of dike found during the Inyo Craters drilling program. Three main fault strands, F_1, F_2, and F_3 occur at the northern end of the Hartley Springs Fault. Fault profiles from Table 2 are numbered in small san serif typeface. Larger numbers next to the profiles are model age (in years) of fault scarp based on use of the *Andrews and Bucknam* [1987] model of fault scarp degradation. Some of the estimated ages suggest the existence of Holocene surface rupture.

eruption, although some of the eruptive events could have occurred decades later than this. Stratigraphic relationships discussed by *Sieh and Bursik* [1986] and *Bailey et al.* [1989] suggest that the length of time between eruption of the airborne tephra from the North Mono and Inyo vents must have been short, perhaps on the order of days. Liquefaction and soft sediment deformation features within the bottom sediments of Mono Lake indicate that a series of

at least five large earthquakes ($M \sim 5.5-6.5$) occurred as the North Mono explosions waned and the Inyo explosions began [*Sieh and Bursik*, 1986]. *Fink* [1985], *Sieh and Bursik* [1986], *Reches and Fink* [1988], and *Mastin and Pollard* [1988] have all speculated that some of the slip on faults in the Inyo domes/Inyo Craters area occurred during this eruptive episode.

[4] The Inyo vents were likely fed from the north trending dike encountered by the Inyo drilling program [*Heiken et al.*, 1988], the Inyo Dike [*Reches and Fink*, 1988]. The dike rock, as well as many of the products of the Inyo eruptions, are geochemically similar to rocks of the Mono Lake islands, indicating a magmatic source within Mono Basin [*Sampson and Cameron*, 1987; *Kelleher and Cameron*, 1990]. Other rocks of the Inyo sequence show a Long Valley affinity [*Sampson and Cameron*, 1987].

[5] The Hartley Springs Fault, a fault of the Sierran range front system, links the trend of the Mono Craters with that of the Inyo Domes (Figure 1). The Inyo Domes are in fact aligned subparallel to the southern part of the fault [*Miller*, 1985]. Within most of the Mono Basin, the locus of diking along the volcanic trend is many kilometers from the range front structure. For example, the Silver Lake Fault is subparallel to the Mono Craters, but lies 10 km to the west. Dike induced deformation on faults in the orientation of the frontal faults is only advantageous within a kilometer or so of the trend of the dike [*Pollard and Segall*, 1987; *Rubin and Pollard*, 1988]. Thus direct mechanical interaction between dikes and most of the range front faults is probably minimal. However, at the southern end of the Hartley Springs Fault, where the trend of the range front structure meets that of the magma system, it is possible that there is direct mechanical interaction between dikes (and eruptions) and the range front fault (and earthquakes).

[6] To understand the possible linkage between the eruptions and earthquakes of 1350 A.D., we undertook a study of the Hartley Springs Fault. This contribution represents a test of the hypotheses that (1) it is geologically and mechanically plausible that a dike triggered slip on the Hartley Springs Fault as the dike approached the fault from the north, and (2) it is mechanically plausible that dike-triggered slip on the Hartley Springs Fault lowered the horizontal compressive stress near the surface along the northern rim of Long Valley caldera, and facilitated the eruptions from the Inyo vents. Testing of these hypotheses consisted of (1) field studies of the Hartley Springs Fault to determine whether it is feasible for slip to have occurred at the time of the eruption, and if so, to constrain the slip magnitude of the rupture, and (2) theoretical calculations to characterize the potential mechanical interaction between the Inyo Dike and the fault.

2. Field Methods and Data

[7] Field work included regional mapping and analyses of the Hartley Springs Fault and other faults in the southernmost Mono Basin. Quaternary fault scarps were mapped. Scarp heights, slope angles and profiles at selected localities along the faults were measured with rod and clinometer or total station geodimeter. Detailed field work entailed constructing topographic and geomorphologic maps of a 200 m $\times$ 400 m area between Glass Creek Flow and Obsidian Flow (Figure 1). We excavated and logged pits, trenches, and roadcuts at this locality, and near the northern end of the Hartley Springs Fault, at Oh! Ridge near June Lake.

2.1. Hartley Springs Fault

[8] Numerous late Quaternary faults and volcanic vents occur along the Sierran range front between June Lake and the northern border of Long Valley Caldera (Figure 1). Most of the faults are short, have small total displacement, and are close to volcanic vents, sometimes in conjugate pairs bounding a graben. These faults may be associated with magmatic activity in the sense that they could be the surface manifestation of the crustal stretching that occurs above a dike at depth [*Hackett et al.*, 1996]. One structure, the Hartley Springs Fault, transects the entire region with a total length of $\sim$8 km as a range-bounding fault. Total vertical movement on the Hartley Springs Fault is probably 420 m since the eruption of 3.23-m.y.-old andesite, and offset rates seem to have increased until approximately 10^5 years ago (Table 1). The Hartley Springs Fault thus has relatively large total displacement, shows evidence of growth behavior, and does not bound a graben. These features are consistent with it being of tectonic origin.

[9] The main strands of the Hartley Springs Fault break late Quaternary deposits at June Lake and Glass Creek. These localities comprise the only places along the range front escarpment that afford some protection from the vast quantities of recently erupted pumice on the escarpment face. Careful inspections over the rest of the length of the fault show that the colluvial wedges composed of pyroclastic debris are sufficiently thick and extensive to overlie young, steep scarp slopes. It is therefore difficult to estimate possible timing and slip magnitude of the most recent activity on the fault. *Bursik and Sieh* [1989] concluded that there may have been negligible Holocene displacement on the Hartley Springs Fault based on a qualitative analysis of fault scarp morphology at June Lake. We have more thoroughly analyzed the data for this region, using the semiquantitative scarp morphology techniques developed by numerous workers in the 1980s [*Andrews and Bucknam*, 1987]. Our new results indicate that scarp height-slope angle relationships for the offset moraines at the northern end of the Hartley Springs Fault are consistent with Holocene displacement on one of the major fault strands (Table 2). Scarp midsection slope angles are consistent with a model age for the most recent offset of $\sim$5000 years on F_2 at June Lake, where a 30,000-year-old moraine is broken by the fault (Figure 1). The scarp of F_2 on the 70,000-year-old moraine yields a much older estimated model age, but this may be because the footslope of the scarp is buried in a small pumice plain, the deposits of which completely cover the downdropped portion of the moraine.

[10] The apparent decreasing slip rate (Table 1) and ambiguous geomorphic evidence of latest Quaternary movement along the fault led *Bursik and Sieh* [1989] to hypothesize that extension in the Mono Basin, once accommodated by range front faulting, is now accommodated by the intrusion of dikes. On the other hand, it is well established that dikes can induce slip on planes of suitable orientation and distance from the dike tip [*Pollard and Segall*, 1987]. The Inyo Dike is known to be within 1 km of the surface trace of the fault at Obsidian and Glass Creek

Table 1. Long-term Offset History of the Hartley Springs Fault at Hartley Springs and June Lake[a]

Location	Offset Units	Estimated Ages for Calculation, m.y.	Vertical Offset of Older-Younger Unit, m	Vertical Offset Rate in Time Slice, mm/yr
Hartley Springs	Andesite-Bishop Tuff	3.23[b]–(0.76, 0.79)[c]	420–290	0.053
June Lake	Bishop Tuff-Mono Basin till	(0.76, 0.79)–(0.13, 0.13, 0.22)[d]	290–205	$0.013^{+0.03}_{-0.0}$
June Lake-Hartley Springs	Mono Basin-Tahoe tills	(0.13, 0.13, 0.22?)–(0.055, 0.7, 0.12)[d]	205–64	$2.4^{+11}_{-1.5}$
June Lake	Tahoe till-present	(0.55, 0.07, 0.12)–0	64–0	$0.09^{+0.3}_{-0.4}$

[a]*Bailey et al.* [1976] reported similar offsets for the andesite and Bishop Tuff along the Hartley Springs Fault. Error bars in vertical offset rate are due to reported uncertainties in ages of offset units. Ages of units are reported as (mininum, best estimate, maximum).
[b]*Fullerton* [1986].
[c]*van den Bogaard and Schirnick* [1995].
[d]*Bursik and Gillespie* [1993].

Flows [*Heiken et al.*, 1988; *Reches and Fink*, 1988]. Is more detailed geological and mechanical evidence consistent with the idea that this dike might have triggered recent slip on the Hartley Springs Fault?

2.2. Oh! Ridge

[11] Evidence regarding late Holocene slip of the Hartley Springs Fault is best found near June Lake, at the northern end of the fault. Exposures of faulted Holocene pumice horizons were made at two places along fault strand F_1 (Figure 1). Scarp exposure is better here than along most of the length of the fault because Pleistocene glaciers downcut through the entire Neogene escarpment, leaving no range front slopes down which pumice deposits could slip to cover evidence of faulting.

[12] The Oh! Ridge trench cut across a 3-m-high scarp developed in Tioga ground moraine on the valley floor (Figure 2). Tioga till was present at the bottom of the trench. The entire scarp here is mantled with a 1.5- to 3-m-thick layer of loose Holocene pumice and colluvium derived from pumice. Between the pumice and the subjacent Tioga till is a wedge-shaped deposit of nonpumiceous colluvium with soil horizons developed in it.

[13] The fault zone underlies the lower part of the scarp and consists of five east dipping normal faults. The western three of these faults displace Tioga till but not overlying colluvium and tephras. The eastern two faults (A and B in Figure 2) extend up through the nonpumiceous colluvium and the overlying pumice, with a vertical displacement of about 35 cm (fault A) and 10–15 cm (fault B). Tioga till is internally deformed in the fault zone, with features like the detached clay seams and clay balls of unit 8 within units 7a and 7b implying soft sediment deformation. In contrast, the upward steepening faults A and B have features typical of brittle faulting of dry deposits. On the basis of this geometry we interpret two faulting events, the older of which faulted Tioga till that was still soft and saturated (very soon after deposition). The younger event breaks unit 2 and therefore postdates the pumice eruption responsible for units 3–5. It is not clear whether the fault breaks some part of the soils overlying unit 3. No tephra of the 1350 A.D. eruption was found at this site.

[14] Units 3–5 are volcanic tephra on which the soil of unit 2 is developed. This tephra contains distinct, low-angle cross bedding in unit 3, consistent with deposition from volcanic surge clouds. Unit 5 (a gray, lapilli pumice layer) contained carbon (sample 97JM02), which yielded a date of 1230 ± 50 ^{14}C years B.P. In general, surges do not propagate more than a few kilometers from source. Units 3–5 probably correlate with the South Mono tephra, which is dominated by surge units, and which has been dated elsewhere to 1200 years B.P. [*Bursik and Sieh*, 1989]. The source area for the South Mono tephra is about 6 km from this site. Unit 6 (a nonpumiceous colluvium) also contained datable organic material (sample number 97JM01), which yielded an age of 3320 ± 60 ^{14}C years B.P. Thus results indicate that the Most Recent Event (MRE) was late Holocene (i.e., it displaced a tephra younger than ~1200 years B.P.), but resulted in only ~50 cm of vertical displacement at the trench site. Clearly, most of the 3 m of topographic relief on the fault scarp was formed by earlier (but post-Tioga) faulting event(s) of larger displacement.

[15] Roughly 50 m north of the trench, fault zone F_1 is exposed in a south facing roadcut on the north side of State Highway 158 (Figure 1). This cut is ~7 m high, and exposes nearly three times the stratigraphic thickness as in the trench (Figure 3). The uppermost tephras in the roadcut correlate to those in the trench, based on macroscopic properties; older pumiceous strata on the downthrown block

Table 2. Offsets and Estimated Model Ages for Scarp Profiles on Splays of the Hartley Springs Fault in the June Lake Area[a]

Fault Strand and Profile	Age of Material, years	Vertical Offset, m	Vertical Offset Rate, mm/yr	Dip of Lower Surface, deg	Dip of Upper Surface, deg	Dip of Steepest Segment, deg	Dimensionless Age	Estimated Model Scarp Age, years
F1-1	20–25,000	5.5	0.24	6.7	7	12.7	3.8	24,000
F1-2	70–120,000	20.9	0.30	2	3.8	16.9	0.518	48,000
F2-3	70–120,000	10.7	0.15	1.3	1.1	9.6	2.14	52,000
F2-9	30–40,000	4.2	0.14	3.4	3	13	1.4	5,300
15	20–25,000	1.2	0.05	0.1	0.3	3	27.4	8,100
17	20–25,000	2.8	0.12	0.1	0	7.8	3.06	5,100
20	30–40,000	3	0.10	0	2.3	7.2	5.77	11,000

[a]Estimated model scarp ages are calculated from the data in the above table using the sliding, or linear plus cubic model of *Andrews and Bucknam* [1987]. An estimated value for the slope diffusivity of 4.7×10^{-3} m^2/yr was used, based on fitting of a linear model to the moraine data from *Bursik* [1989] for the nearby moraines of Lee Vining Canyon. Age of material (offset till) from *Bursik and Gillespie* [1993]. Best estimates were used for vertical offset rate calculations, which are, from youngest to oldest tills shown, 23,000 years, 30,000 years, and 70,000 years.

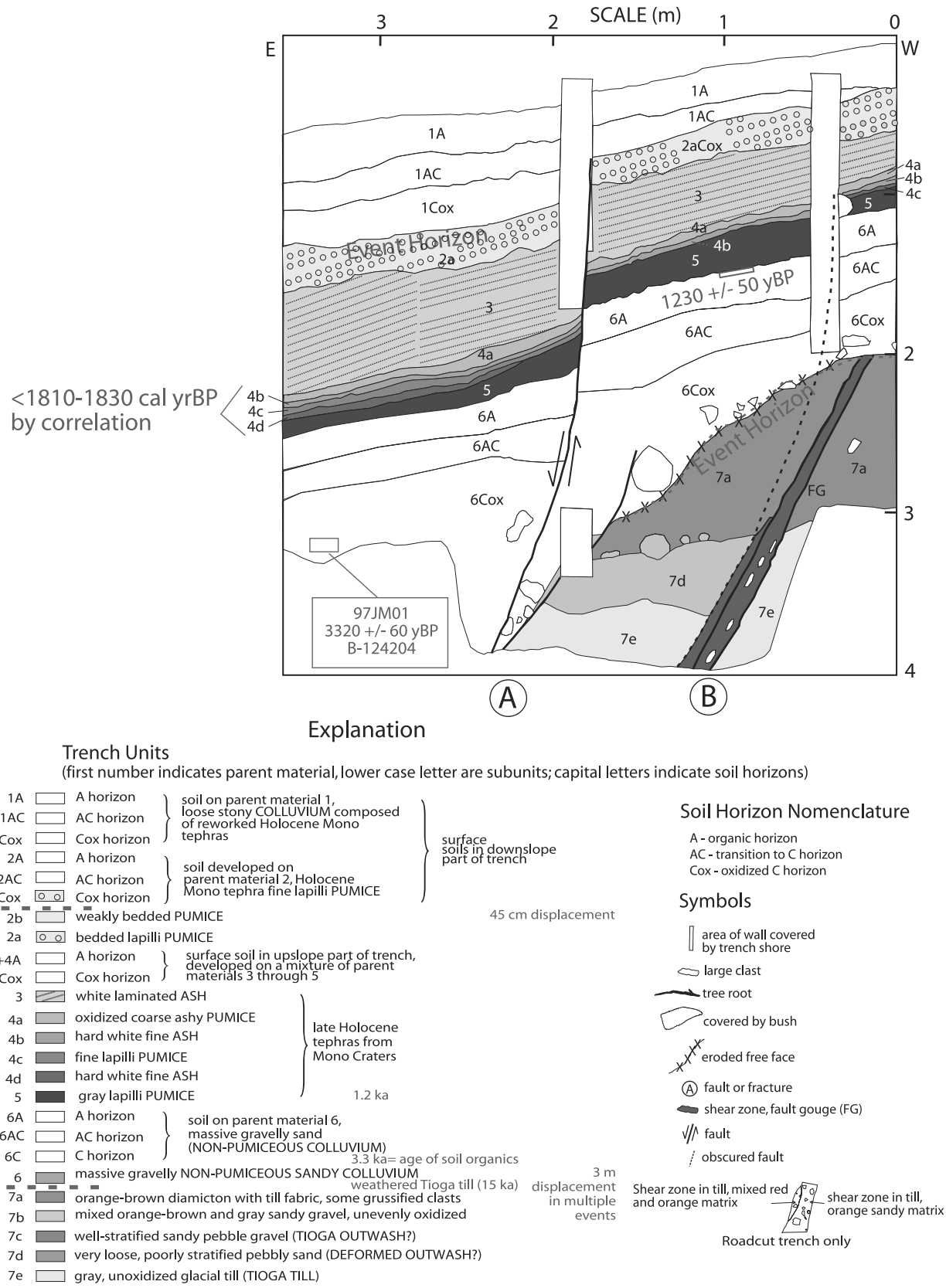

Figure 2. Log of trench near Oh! Ridge, at the northern end of the Hartley Springs Fault. The figure shows a detail of the entire cut, which was 28 m long. Not all of the units shown in the Explanation occur in this detailed view. Relationships in the excavation show that faulting occurred on the Hartley Springs Fault after 1200 years B.P. See color version of this figure in the HTML.

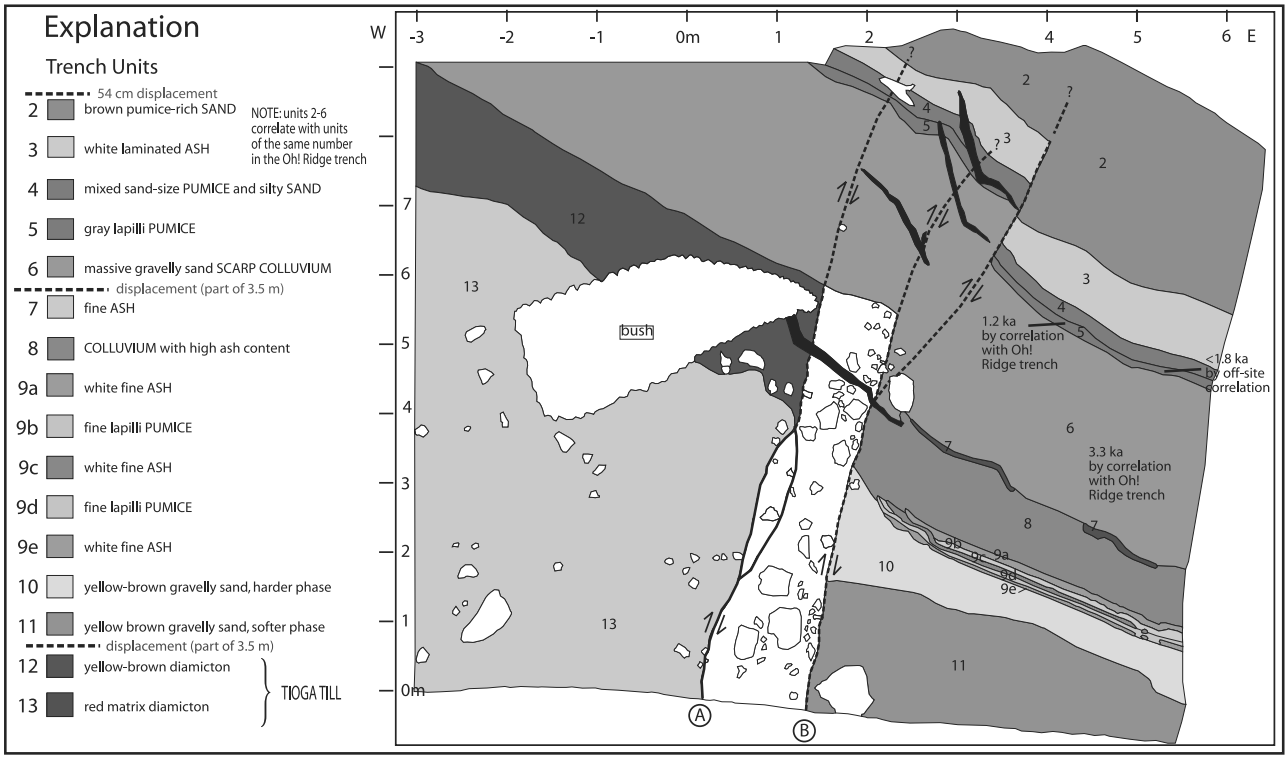

Figure 3. Log of cleared roadcut along Highway 158 on the flank of the Oh! Ridge scoria cone. Relationships in the roadcut are consistent with those seen in the Oh! Ridge trench. See color version of this figure in the HTML.

evidently do not have counterparts in the Oh! Ridge trench. Most of the Tioga till on the upthrown block has a matrix with a reddish purple color. This till was derived from glacial erosion into the southern flank of the nearby Oh! Ridge scoria cone.

[16] The fault is a 0.6-m-wide shear zone that juxtaposes Tioga till (on the west) against ash- and pumice-rich colluvium. The fault zone has a steep dip to the west (Figure 3), which is opposite to the dip expected for a down-to-the-east normal fault. There are two possible explanations for this dip: (1) it represents near-surface fault refraction, a phenomenon often seen as extensional faults approach the ground surface or (2) the fault may have a significant lateral component of slip, and the west dip is similar to a flower structure where fault strands diverge and "roll over" as they approach the surface.

[17] The traces of the faults are obscure where they penetrate massive unit 6 (gravelly sand with a low pumice content, probably slope colluvium), but vertical displacements are measurable in better stratified units 5, 4, and 3. The eastern splay of fault B has a vertical displacement of 43 cm and the western splay has a down-to-the east warp of ~11 cm (note that the apparent displacements shown on the log are slope distances, and must be reduced by the sine of 35°). This total vertical displacement of ~54 cm in units 2–6 is similar to the total vertical displacement (45–50 cm) of the same units in the Oh! Ridge trench. Tioga till exposed on the upthrown block is displaced down-to-the-east at least 2.7 m, because it is not exposed on the downthrown side of the fault. This roadcut does not yield evidence for any additional events beyond those interpreted from the June Lake trench, i.e., one Holocene event, and another post-Tioga event(s) of larger displacement.

[18] The exposures near June Lake thus yield evidence for ~50 cm of vertical displacement after 1200 years B.P. at the northern end of the Hartley Springs Fault. Relationships near Glass Creek, closer to the southern end of the fault, are used to determine if some of this slip occurred about the time of the Inyo and North Mono eruptions.

2.3. Glass Creek Embayment

[19] The range front along the trend of the Hartley Springs Fault is embayed where it is crossed by Glass Creek. The embayment may be the result of erosion of the range front escarpment by Glass Creek in the past. Since then, Glass Creek has followed a variety of courses within the embayment as indicated by the existence of numerous abandoned landforms. Remnants of five planar to subplanar surfaces occur within the embayment (Figure 4). Their relative distance from the modern course of Glass Creek and their internal stratigraphy suggest that most of the surfaces are stream terraces and that they young from surface I to surface V. Surface I is directly underlain by volcaniclastic material; all others are directly underlain by material of fluvial origin. Detailed interpretations of these surfaces are discussed in other works [*Bursik and Reid*, 1999, also manuscript in preparation, 2002].

[20] A lineament (F_1) can be followed from the small dome at Glass Creek, across surface I, where it is expressed as a depression, then between surfaces II and III. The lineament is collinear with the trend of the range front escarpment of the Hartley Springs Fault to the north and

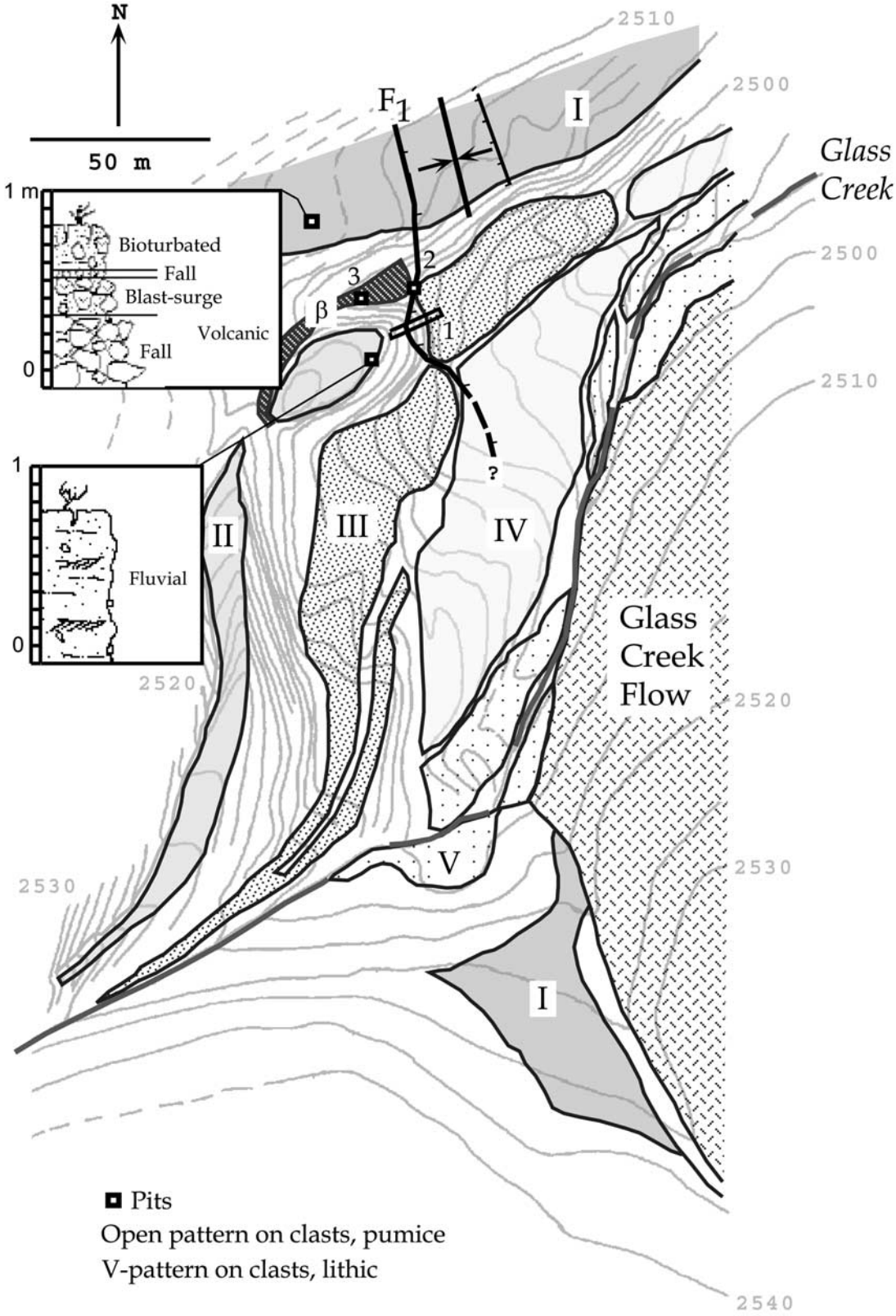

Figure 4. Topographic and geomorphic map of the fluviovolcanic surfaces at Glass Creek. The different surfaces, channel β (other paleochannels exist but are not labeled), and the fault scarp are shown. Line surround by two arrows point inward represents axis of swale. Roman numerals refer to surface number; lowercase Greek letters designate channels. There are remnants of five surfaces, and four channels and paleochannels of Glass Creek.

south of the embayment (Figures 1 and 4). The alignment with the Hartley Springs Fault, downsag in surface I, crosscutting geomorphic pattern with respect to the surfaces, and apparent offset between surfaces II and III are all consistent with the lineament being a fault scarp. To observe potential offset of units across the fault, pits were dug across and near the scarp. (Trenching was attempted but a backhoe could not make it to the site.)

[21] Pit 1 (Figures 4 and 5) was dug from surface III across the surface II riser. Within both surfaces, the excavation revealed horizontal pyroclastic layers of the Inyo sequence underlying fluvial sands and gravels. Clasts in surface II alluvium are primarily granular sands of redeposited Inyo pyroclasts, while those in surface III alluvium are basement granitic and older volcanic rocks.

[22] Pit 3, dug in the channel (β) northwest of pit 1, uncovered alluvium (unit 3) similar to the alluvium forming the lower strata of surface III at pit 1 (Figure 5). A topographic profile constructed downchannel from pit 3 revealed a steep slope segment within the channel floor where it meets surface III (Figure 5). This steep slope segment is interpreted as an eroded fault scarp, and its height is consistent with a vertical offset of 1 m. Pit 2, 2 m long in the cross-lineament direction, was dug into the center of this steepest slope segment. The upper surface of a bouldery facies in unit 3 was 0.2 m higher on the upstream side of the steepest slope segment of the scarp than on the downstream side. Pebble imbrication directions in unit 3 are consistent with flow downchannel at the time of formation of the steep slope segment, as opposed to across surface III. The geomorphic and stratigraphic data are consistent with, although not sufficiently clear to prove the occurrence of, an earthquake along the Hartley Springs Fault after the formation of surface III.

[23] The alluvial units underlying surface II overlie pyroclastic units. Because these are the highest pyroclastic units associated with the Inyo eruptions, and because of the presence of both rhyolite and rhyodacite components, they must represent the near-vent Glass Creek tephra, which was the last tephra erupted during the Inyo sequence [*Miller*, 1985]. Thus at least some faulting is contemporaneous with or postdates the pyroclastic phases of the Inyo eruption. This particular event (and terrace formation) may have preceded emplacement of the Glass Creek Flow, as talus deposits derived from the flow overlie surface V (although these talus deposits could postdate emplacement of the flow).

[24] The maximum total dip-slip movement recorded on fault F_1 at Glass Creek is ~1.0 m, based on the apparent geomorphic offset. The apparent vertical separation of the upper contact of unit 3 may provide an estimate of minimum dip-slip movement during the most recent event because the base of the unit is not exposed, and the deposit on the downdropped side could be colluvium derived from unit 3. The estimated minimum dip-slip movement is therefore ~0.2 m. Surface slip magnitudes are highly variable along the length of any rupture zone [*Sieh*, 1981], but are generally greatest near the center of the zone and drop to zero at the ends. Because the Glass Creek site is less than 2 km from the southern termination of the fault, the slip is likely not a maximum for the possible event recorded there. At Oh! Ridge, the 50 cm of slip occurring since 1200 years B.P. could represent a total from the five events at the time of the 1350 A.D. eruption [*Sieh and Bursik*, 1986], or even include other, earlier events. The Oh! Ridge sites are at the northern termination of the fault. Although there are several ambiguities in interpretation, it is possible to say that the data are consistent with the hypotheses that 0.2 m to 1.0 m of mean slip occurred on the Hartley Springs Fault in a single event, and that more than 0.5 m of mean slip occurred in numerous events at the time of the 1350 A.D. eruption.

2.4. Estimated Earthquake Size

[25] To obtain a rough estimate of minimum earthquake magnitude during a single event, we use the geomorphic and stratigraphic discontinuities to limit mean slip during an earthquake on the Hartley Springs Fault. If the fault can be represented by a plane, extending to a depth of 10 km [*Smith and Bruhn*, 1984], dipping at an angle of 60°, for a total width, W, of 11 km and length, L, of 8 km (between the northern rim of Long Valley Caldera and the end of the splays in the June Lake area [*Bursik and Sieh*, 1989], then the seismic moment, M_0, for the offset event can be estimated using [*Hanks et al.*, 1975]

$$M_0 = \mu s L W, \tag{1}$$

where μ, the shear modulus, is assumed to have a value of 33 GPa. The moment has a value of $0.66–2.9 \times 10^{18}$ N m, for bracketing values for slip of 0.2 and 1.0 m, respectively. The associated moment magnitude can be calculated as [*Hanks and Kanamori*, 1979]:

$$M_w = 2/3 \log 10 M_0 - 3.7, \tag{2}$$

yielding M_w 5.9–6.3. An event of this size on the Hartley Springs Fault is likely just capable of creating the liquefaction structures observed by *Sieh and Bursik* [1986] in the lacustrine deposits of Mono Lake.

3. Quantitative Model of Dike-Fault Coupling

[26] We now further investigate the relationships between the Mono Craters eruptions, earthquakes on the Hartley Springs Fault, and the Inyo eruptions of approximately 1350 A.D. by developing a quantitative model for the evolution of progressive diking and faulting events. *Bursik and Sieh* [1989] suggested that a magma chamber underlying the Mono Basin was overpressured at the time of the North Mono eruption of 1350 A.D. in the sense that the pressure within the chamber was above the normal stress across potential fracture planes subparallel to the range front fault system. If so, the overpressured magma could feed the propagation of a south directed dike, such as the Inyo Dike [*Reches and Fink*, 1988]. *Reches and Fink* [1988] constrained the Inyo Dike to have general characteristics consistent with those where it was encountered between Glass Creek and Obsidian Flows during the Inyo drilling program [*Heiken et al.*, 1988]. This dike would have propagated from a magma chamber in the Mono Basin, given its geochemical affinity with the rocks of the Mono Lake islands, southward toward the Hartley Springs Fault. It may have taken advantage of planes of weakness that had developed in association with the eruption of Wilson's Butte (Figure 1) 1200 years B.P. [*Miller*, 1985]. The dike would have been perhaps 5–10 m wide through most of its depth [*Heiken et al.*, 1988; *Bursik and Sieh*, 1989].

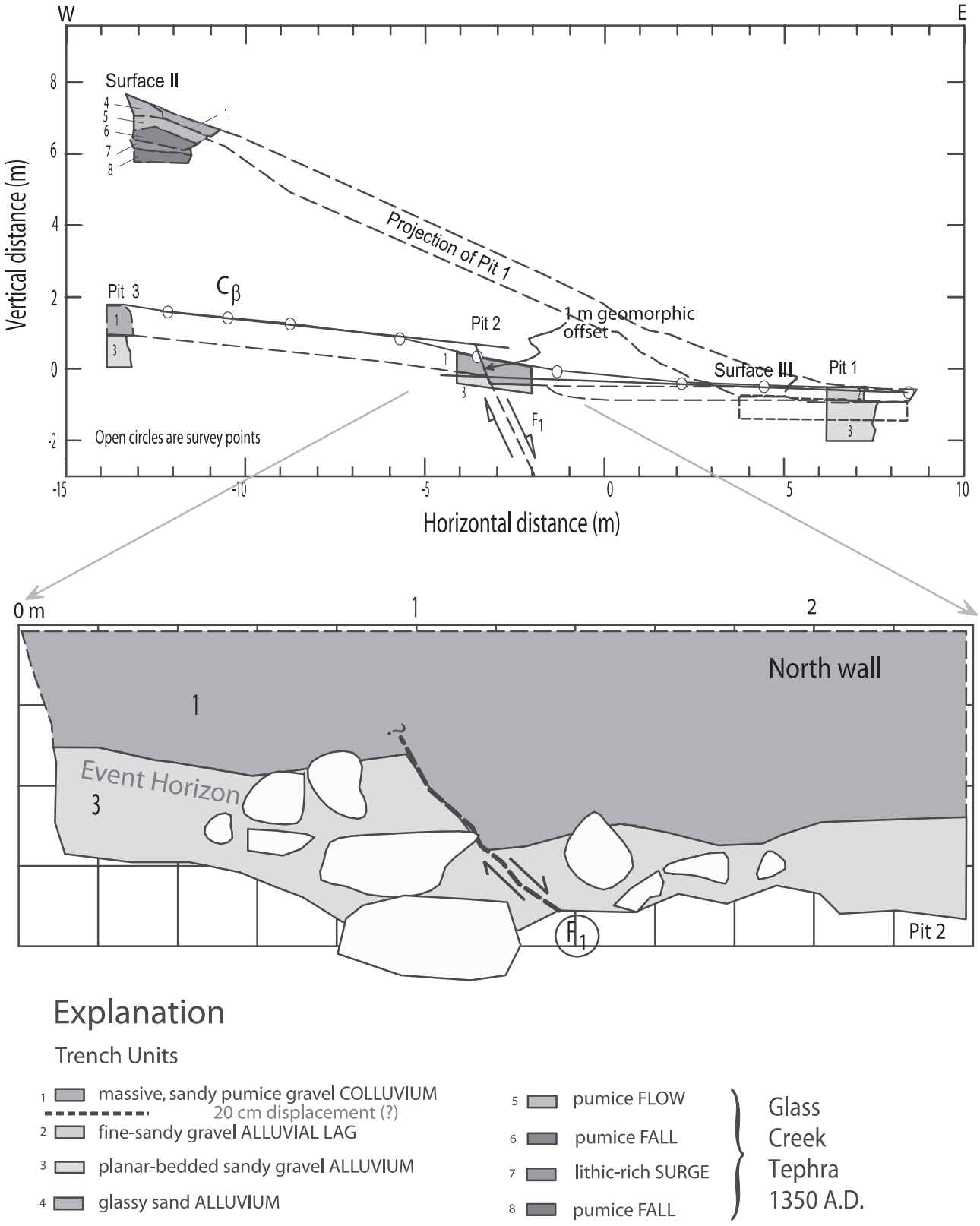

Figure 5. (top) Fault scarp profile (open circles) and cross section along the floor of Channel beta (β) to surface III, with pit 1 projected onto the same plane. Unit contacts (within pits excavated on surface III and at the base of β) are solid where measured and dashed where inferred between pits. (bottom) An expanded view of the units in pit 2. Fault plane is inferred. See color version of this figure in the HTML.

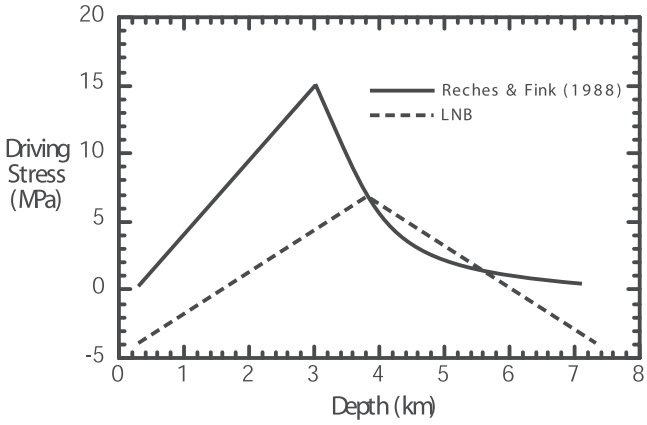

Figure 6. Driving pressures as a function of depth in the dike used in the numerical calculations. Solid line shows model of *Reches and Fink* [1988], while dashed line is that predicted by the LNB model using a density contrast between the magma and host rock of 300 kg/m^3.

[27] We hypothesize that the stress perturbations associated with the southward propagating Inyo Dike were sufficient to induce slip along the Hartley Springs Fault. Furthermore, we hypothesize that slip along the fault, in turn, perturbed the stress field near the southern termination of the dike, creating zones of reduced horizontal confining stress that would enable migration of magma from the Long Valley chamber and provide sites for the major vents and domes of the Inyo sequence.

[28] To test these hypotheses, we determined the stress perturbations induced by a southward propagating dike from the Mono Basin magma chamber using a three dimensional boundary element model for a linear elastic half-space [*Thomas and Pollard*, 1993]. In the model, we idealized the Inyo Dike as a vertical, north-south trending mode I displacement discontinuity. The model dike has a height of 7 km and extends to within 0.3 km of the surface. Following the analysis of *Reches and Fink* [1988], we assume that the driving pressure of the Inyo Dike (magma pressure plus the least compressive horizontal stress, where compression is negative) reached a maximum magnitude of 15 MPa at a depth of 3 km and varied as a function of depth (Figure 6). To investigate the sensitivity of our results to the

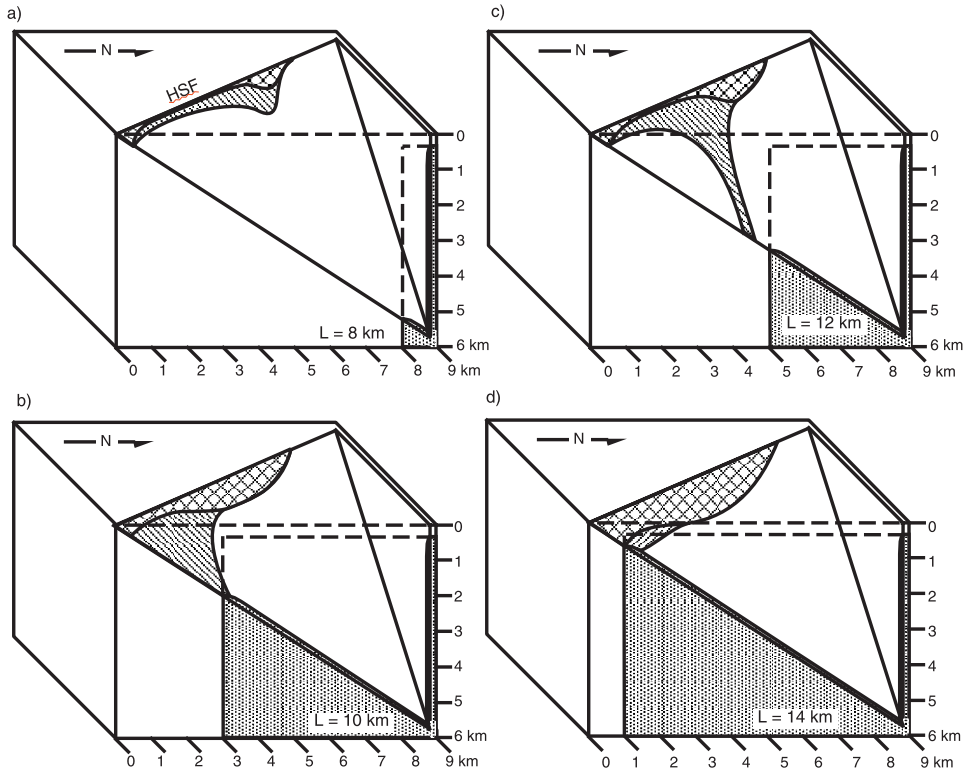

Figure 7. Regions of potential fault slip (calculated using equation (3)) induced by the southward propagation of the Inyo Dike from the Mono Basin as a function of length *L* of the dike.(a) Dike length 8 km, (b) dike length 10 km, (c) dike length 12 km, and (d) dike length 14 km. On top surface, solid line indicates trend of the Hartley Springs Fault; dashed line represents trend of the Inyo Dike. Stippled area on front surface represents Inyo Dike. Rightward dipping diagonal line patterns indicate regions of potential slip predicted using the driving pressure model of *Reches and Fink* [1988], leftward dipping diagonal line patterns indicate regions of potential slip predicted using the LNB driving stress model, cross-hatched patterns indicate regions of potential slip predicted by both models. Distance is measured southward from an origin underneath the central Mono Craters. Obsidian Flow would lie at the southern tip of the 10-km-long dike (Figure 7b).

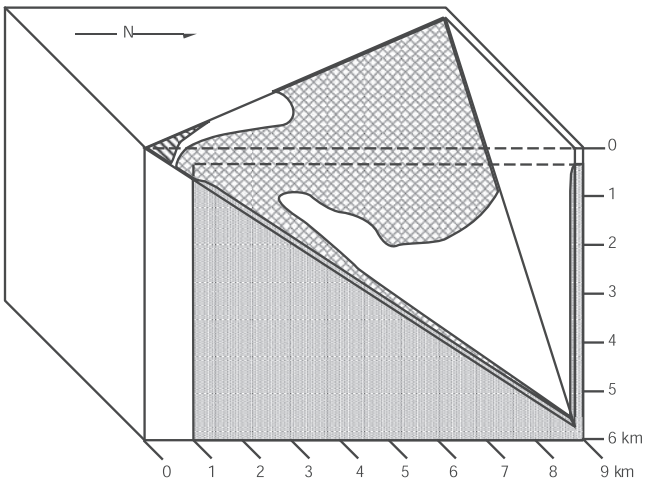

Figure 8. Detail of potential slip regions for $L = 14$ km and increased pore fluid pressure to 0.52× lithostatic pressure. Driving pressure model of *Reches and Fink* [1988] is assumed. Angled line region on fault plane is in compression. Distances on edge of block are in km. Compare to Figure 7d.

assumed driving stress distribution, we also consider the driving stress variation predicted by the level of neutral buoyancy (LNB) driving stress model [*Lister*, 1990; *Fialko and Rubin*, 1999]. Following *Reches and Fink* [1988], we assume that the ratio of horizontal principal stresses at the time of dike emplacement was 0.6 and that the least compressive horizontal principal stress is equal to 0.75 times the lithostatic stress and oriented normal to the dike. The model dike extends laterally to 15 km due north of the surface intersection of its trend and that of the Hartley Springs Fault. The intersection is just south of Glass Creek Flow. The trend of the model Hartley Springs Fault is N23°W, and the fault extends 9.5 km NNW from its intersection with the trend of the Inyo Dike. Unless otherwise noted, the fault is assumed to dip 60° to the east. The linear elastic half-space is assumed isotropic with a shear modulus, $G = 20$ GPa [*Birch*, 1966], and Poisson's ratio $\nu = 0.1$ [*Reches and Fink*, 1988]. Lithostatic stress is calculated assuming an average rock density of 2670 kg/m^3. The dike and fault were discretized into boundary elements with linear dimensions no larger than 0.5 km. To determine if the stress perturbation induced by the propagating dike could induce slip along the Hartley Springs Fault, we assume that slip along the fault occurs when $\Delta\tau > 0$, where $\Delta\tau$ is given by the Mohr-Coulomb failure criterion:

$$\Delta\tau = |\tau| + \mu_f(\sigma_n + p_h), \tag{3}$$

where τ and σ_n are the resolved maximum shear and normal tractions along the Hartley Springs Fault plane, μ_f is the coefficient of friction (assumed equal to 0.5) [*Byerlee*, 1978] and p_h is the pore pressure (unless otherwise stated, assumed to be hydrostatic). The regions of potential fault slip along the dipping fault plane ($\Delta\tau > 0$), for various lengths L of the vertical propagating dike, are shown in the block diagrams of Figure 7. Average excess shear stress magnitudes $\Delta\tau$ within the regions of potential slip range from 0.5 to 4 MPa for dike lengths from 8 to 14 km; maximum $\Delta\tau$ magnitudes range from 2 to 8 MPa for the same range of dike lengths. These excess shear magnitudes are similar to the typical shear stress drop of large earthquakes [*Stein et al.*, 1994]. The calculations suggest that for dike lengths greater than 8 km, the stress perturbations associated with the southward

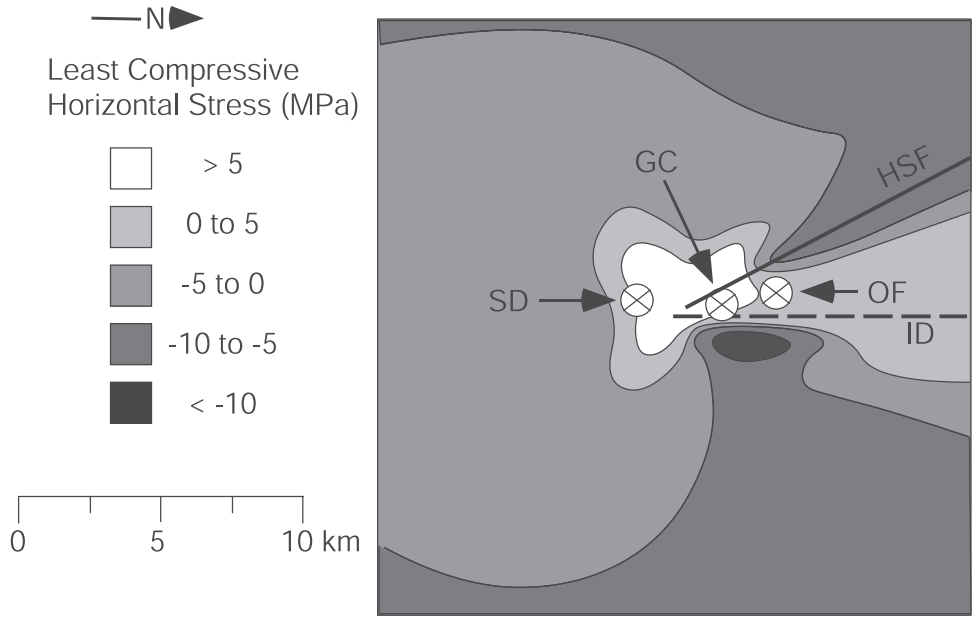

Figure 9. Contours of the magnitude of the least compressive principal stress near the southern termination of the Hartley Springs Fault (HSF) and Inyo Dike (ID) after 1 m of slip along the fault. The driving pressure model of *Reches and Fink* [1988] is used and $L = 14$ km. Circled cross indicates locations of, from north to south, Obsidian (OF), Glass Creek (GC), and South Deadman (SD) Flows.

propagation of the Inyo Dike could have induced slip along the Hartley Springs Fault. In other words, as the dike approached the fault from the north along the locus of the southern Mono Craters vents and Wilson's Butte, it could induce slip on the fault once it propagated sufficiently close, even if the fault were not in a state advantageous for slip before its approach. Further examination of the results reveals that failure results from increased shear stress along the fault rather than the reduction of fault normal stress.

[29] For shorter dike lengths, the regions of potential slip are greater for the driving stress model of *Reches and Fink* [1988] than for the LNB model. However, as the dike approaches the fault, the differences between the two models are relatively minor. Hence in the following treatment, we only consider the model of *Reches and Fink* [1988].

[30] The optimal dike length for inducing slip along the Hartley Springs Fault (i.e., the length associated with the largest potential slip patch) is ~14 km (Figure 7d). At this length, the failure criterion is satisfied to depths of 2–3 km where the fault plane intersects the dike. The cross-hatching in Figure 7 only indicates regions where the failure criterion is satisfied prior to any slip on the fault. Once slip initiates within these regions, the stress perturbation induced by the slip will likely allow slip to occur along the fault outside of these initial failure patches. Thus the size of the failure patches shown in Figure 7 do not correspond to the region over which failure could occur once slip initiated. It is likely that the region of the fault that would slip during an earthquake is larger than shown in these figures.

[31] The size of the potential slip patches is sensitive to the assumed pore pressure and fault orientation. Heat derived from the magma in the propagating dike most likely increased pore pressures surrounding the dike. Where the fault is near the dike, this increased pore pressure increases the likelihood of slip along the fault (equation (3)). For example, Figure 8 shows the potential failure patch for L = 14 km, assuming the ratio of fluid to lithostatic pressure equals 0.52. For reference, under hydrostatic conditions, the ratio of fluid to lithostatic pressure equals 0.37. Comparing Figures 7d and 8 demonstrates that fluid overpressuring significantly increases the size of the region satisfying the failure criterion along the fault. Any fluid leakage from the dike into the fault plane where the two intersect would similarly increase the region of potential slip. As with a steeply dipping fault, the lateral extent of potential slip along a vertical fault (not illustrated) is typically 5 to 7 km. This is in good accord with the modern-day surface expression of the fault (~8 km).

[32] Once the Hartley Springs Fault slipped, the stress perturbations induced by the slip would affect the further propagation of the Inyo Dike. To examine this possibility, the three-dimensional boundary element model was used to determine the stress field in a region near the southern end of the Hartley Springs Fault after 1 m of right-lateral and dip-slip motion along the fault. Figure 9 is a contour plot of the magnitude of the least principal horizontal stress following slip on the Hartley Springs Fault at a depth corresponding to the top of the dike (0.3 km). Slip along the fault induces a region of reduced compressive stress near the surface intersection of the trends of the dike and the fault. The region of the reduced compressive stress is well correlated with the locations of the three Inyo domes. This suggests that the mechanical interaction of the Inyo Dike and the Hartley Springs Fault may have locally reduced the horizontal confining stress and allowed the dike to propagate to the surface, creating the major vent sites that were eventually occupied by the extrusive domes, and perhaps drawing magma from an otherwise inactive Long Valley chamber. Without the induced slip on the fault, these zones of reduced confinement would not occur, making it more difficult for the dike to find a pathway to the surface.

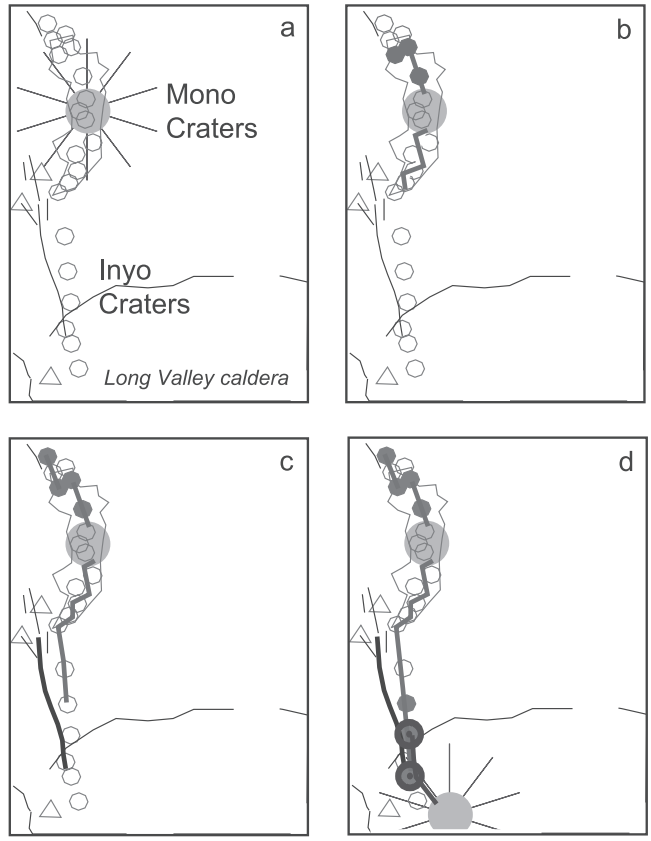

Figure 10. Schematic map sequence (Figures 10a–10d) illustrating the progression of eruptive and faulting events at the time of the North Mono (Figure 10b) and Inyo (Figure 10d) eruptions. (a) Unrest of magma body in Mono Basin, (b) dike injection from Mono Basin magma body and early North Mono eruptions, (c) continued North Mono eruptions and injection of Inyo Dike southward with initial earthquakes on Hartley Springs Fault, and (d) injection of Inyo Dike to its southernmost extent and dike from Long Valley northward, with Inyo eruptions and continued eruptions of Mono Craters. See color version of this figure in the HTML.

4. Conclusions

[33] Our results suggest that a volcanotectonic "cascade" of eruptive and faulting events is a possible mechanism by

which a large section of the range front system becomes activated (Figure 10). In the kinematic interpretation of fault and dike relationships between the Mono and Inyo chains and the range front fault system, *Bursik and Sieh* [1989] hypothesized that either dikes or faults accommodated regional extension at any one position along the Sierran range front. The present mechanical analysis of dike propagation suggests that the relationship between the two mechanisms is somewhat more complicated, and that the two mechanisms for accommodation of crustal stretching might interact locally.

[34] The sequence of volcanic and tectonic events of 1350 A.D. in the Mono/Inyo Craters area are recorded in the landforms and strata at June Lake, and at the juncture of the Hartley Springs Fault and Glass Creek. The stratigraphy at June Lake and Glass Creek, coupled with that found in Mono Lake, is consistent with the interpretation that explosive events of the North Mono and Inyo eruption sequences were accompanied by a series of strong earthquakes, which were likely along the Hartley Springs Fault. Our results indicate that the earthquakes may have been triggered by emplacement of a dike close to the fault. Movement on the fault, in turn, created regions of low confining stress within which magma could preferentially be drawn and erupt. These low confinement zones may have drawn magma both from the dike propagating from the Mono Basin as well as from the otherwise moribund Long Valley magma chamber.

[35] There are implications of the present work for the ongoing monitoring effort in Long Valley caldera, and for the development of volcanic and tectonic activity in range front and rift environments. The possibility that a future eruption from the Long Valley magmatic system could be triggered by tectonic activity adjacent to the caldera, either to the north or south, needs to be carefully considered. If magma is close to a fault termination, and there is enough slip on the fault to create zones of sufficiently low pressure, then it is possible that earthquake activity similar to that observed in 1980 along the Hilton Creek Fault to the south of the caldera (four M 6 earthquakes) could induce eruption.

[36] The disposition of faults and volcanoes in the Mono Basin and Long Valley Caldera is similar to that in many other range front and rift areas throughout the world, including much of the Basin Ranges, Iceland, Ecuador, and Afar [*Rubin and Pollard*, 1988; *Bailey et al.*, 1989]. It is therefore possible that a volcanotectonic cascade of activity, at least as extensive as that discussed in the present contribution, could develop in many other areas.

[37] **Acknowledgments.** Discussions with Carol Prentice and John Reid in the field are gratefully acknowledged. Amy K. Friends assisted with much of the field work, and George Bursik and several volunteers with the Mammoth district fire fighting brigade were helpful in mapping and excavation at Glass Creek. At Oh! Ridge, help of field assistants Molly Bentley and Jason Amato and collaboration with Andre Sarna-Wojcicki are acknowledged. Work was supported by NEHRP grant 1343-HQ-97-GR-03022, and in part by NASA grants NAG52273 and NAG53142. Reviews by Yuri Fialko, an anonymous reviewer, and by Associate Editor Freysteinnn Sigmundsson are gratefully acknowledged. Editors and anonymous reviewers of an earlier, related manuscript are also acknowledged.

References

Andrews, D., and R. Bucknam, Fitting degradation of shoreline scarps by a nonlinear diffusion model, *J. Geophys. Res.*, *92*, 12,857–12,867, 1987.

Bailey, R. A., G. B. Dalrymple, and M. A. Lanphere, Volcanism, structure, and geochronology of Long Valley Caldera, Mono County, California, *J. Geophys. Res.*, *81*, 725–744, 1976.

Bailey, R. A., C. D. Miller, and K. E. Sieh, Long Valley caldera and Mono-Inyo Craters volcanic chain, eastern California, in *Field Excursions to Volcanic Terranes in the Western United States*, vol. II, *Cascades and Intermountain West*, edited by C. E. Chapin and J. Zidek, *Mem. N.M. Bur. Mines Miner. Resour.*, *47*, 227–254, 1989.

Birch, F., Compressibility: Elastic constants, in *Handbook of Physical Constants*, pp. 107–173, Geol. Soc. of Am., Boulder, Colo., 1966.

Bursik, M. I., Late Quaternary volcano-tectonic evolution of the Mono Basin, eastern California, Ph.D. thesis, 293 pp., Calif. Inst. of Technol., Pasadena, 1989.

Bursik, M. I., and A. R. Gillespie, Late Pleistocene glaciation of Mono Basin, California, *Quat. Res.*, *39*, 24–35, 1993.

Bursik, M. I., and J. B. Reid, Lahars in Glass Creek and Owens River during the Inyo eruption, Long Valley caldera, CA, *Eos Trans. AGU*, *80*(46), Fall Meet. Suppl., F1187, 1999.

Bursik, M., and K. E. Sieh, Range front faulting and volcanism in the Mono basin, eastern California, *J. Geophys. Res.*, *94*, 15,587–15,609, 1989.

Byerlee, J., Friction of rocks, *Pure Appl. Geophys.*, *116*, 615–626, 1978.

Fialko, Y. A., and A. M. Rubin, What controls the along-strike slopes of volcanic rift zones?, *J. Geophys. Res.*, *104*, 20,007–20,020, 1999.

Fink, J., Geometry of silicic dikes beneath the Inyo Domes, California, *J. Geophys. Res.*, *90*, 11,127–11,133, 1985.

Fullerton, D., Chronology and correlation of glacial deposits in the Sierra Nevada, California, *Quat. Sci. Rev.*, *5*, 161–167, 1986.

Hackett, W. R., S. M. Jackson, and R. P. Smith, Paleoseismology of volcanic environments, in *Paleoseismology*, *Int. Geophys. Ser.*, vol. 62, edited by J. P. McCalpin, pp. 147–181, Academic, San Diego, Calif., 1996.

Hanks, T., and H. Kanamori, A moment magnitude scale, *J. Geophys. Res.*, *84*, 2348–2350, 1979.

Hanks, T., J. Hileman, and W. Thatcher, Seismic moments of the larger earthquakes of the southern California region, *Geol. Soc. Am. Bull.*, *86*, 1131–1139, 1975.

Heiken, G., K. Wohletz, and J. Eichelberger, Fracture fillings and intrusive pyroclasts, Inyo domess, California, *J. Geophys. Res.*, *93*, 4335–4350, 1988.

Hill, D., A model for earthquake swarms, *J. Geophys. Res.*, *82*, 1347–1352, 1977.

Kelleher, P. C., and K. L. Cameron, The geochemistry of the Mono Craters-Mono Lake islands volcanic complex, eastern California, *J. Geophys. Res.*, *95*, 17,643–17,659, 1990.

Lister, J., Buoyancy-driven fluid fracture: Similarity solutions for the horizontal and vertical propagation of fluid-filled cracks, *J. Fluid Mech.*, *217*, 213–239, 1990.

Mastin, L., and D. Pollard, Surface deformation and shallow dike intrusion processes at Inyo Craters, Long Valley, California, *J. Geophys. Res.*, *93*, 13,221–13,235, 1988.

Miller, C. D., Holocene eruptions at the Inyo volcanic chain, California; implications for possible eruptions in Long Valley Caldera, *Geology*, *13*, 14–17, 1985.

Pollard, D., and P. Segall, Theoretical displacements and stresses near fractures in rock; with applications to faults, joints, veins, dikes, and solution surfaces, in *Fracture Mechanics of Rock*, edited by B. Atkinson, pp. 277–349, Academic, San Diego, Calif., 1987.

Reches, Z., and J. Fink, The mechanism of intrusion of the Inyo Dike, Long Valley Caldera, California, *J. Geophys. Res.*, *93*, 4321–4334, 1988.

Rubin, A. M., and D. D. Pollard, Dike-induced faulting in rift zones of Iceland and Afar, *Geology*, *16*, 413–417, 1988.

Rundle, J. B., and D. P. Hill, The geophysics of a restless caldera: Long Valley, California, *Annu. Rev. Earth Planet. Sci.*, *16*, 251–271, 1988.

Sampson, D. E., and K. L. Cameron, The geochemistry of the Inyo volcanic chain; multiple magma systems in the Long Valley region, eastern California, *J. Geophys. Res.*, *92*, 10,403–10,421, 1987.

Savage, J. C., and M. M. Clark, Magmatic resurgence in Long Valley Caldera, California; possible cause of the 1980 Mammoth Lakes earthquakes, *Science*, *217*, 531–533, 1982.

Sieh, K., A review of geological evidence for recurrence times of large earthquakes, in *Earthquake Prediction: An International Review*, *Maurice Ewing Ser.*, vol. 4, edited by D. W. Simpson and P. G. Richards, pp. 181–207, AGU, Washington D. C., 1981.

Sieh, K., and M. I. Bursik, Most recent eruption of the Mono Craters, eastern central California, *J. Geophys. Res.*, *91*, 12,539–12,571, 1986.

Smith, R., and R. Bruhn, Intraplate extensional tectonics of the eastern Basin-Range: Inferences on structural style from seismic reflection data, regional tectonics and thermal-mechanical models of brittle/ductile deformation, *J. Geophys. Res.*, *89*, 5733–5762, 1984.

Stein, R., G. King, and K. Lin, Stress triggering of the 1994 *M*6.7 Northridge, California, earthquake by its predecessors, *Science*, *265*, 1432–1435, 1994.

Thomas, A. L., and D. D. Pollard, The geometry of echelon fractures in rock: Implications from laboratory and numerical experiments, *J. Struct. Geol.*, *15*, 323–334, 1993.

van den Bogaard, P., and C. Schirnick, $^{40}Ar/^{39}Ar$ laser probe ages of Bishop Tuff quartz phenocrysts substantiate long-lived silicic magma chamber at Long Valley, United States, *Geology*, *23*, 759–762, 1995.

Vetter, U., Focal mechanisms and crustal stress patterns in western Nevada and eastern California, *Ann. Geophys.*, *2*, 699–710, 1984.

M. Berry, 29045 Douglas Park Road, Evergreen, CO 80439, USA. (berryme@earthlink.net)

M. Bursik, Department of Geology, 876 Natural Sciences, State University of New York at Buffalo, Buffalo, NY 14260, USA. (mib@geology. buffalo.edu)

J. McCalpin, GEO-HAZ Consulting, Inc., Crestone, CO 81131, USA. (mccalpin@geohaz.com)

C. Renshaw, Department of Earth Sciences, Dartmouth College, Hanover, NH 03755, USA. (carl.e.renshaw@dartmouth.edu)